View metadata, citation and similar papers at core.ac.uk

brought to you by CORE

provided by Elsevier - Publisher Connector

Biochimica et Biophysica Acta 1847 (2015) 1119–1128

Contents lists available at ScienceDirect

Biochimica et Biophysica Acta

journal homepage: www.elsevier.com/locate/bbabio

Effects of the protonophore carbonyl-cyanide m-chlorophenylhydrazone on intracytoplasmic membrane assembly in *Rhodobacter sphaeroides*

Kamil Woronowicz, Oluwatobi B. Olubanjo, Daniel Sha, Joseph M. Kay, Robert A. Niederman *

Department of Molecular Biology and Biochemistry, Rutgers Energy Institute, Rutgers University, Busch Campus, Piscataway, NJ 08854-8082, USA

ARTICLE INFO

Article history:
Received 17 March 2015
Received in revised form 2 June 2015
Accepted 3 June 2015
Available online 5 June 2015

Keywords:
Bacterial photosynthesis
Light-harvesting
Reaction center
ATPase
Transhydrogenase
Membrane assembly

ABSTRACT

The effect of carbonyl-cyanide m-chlorophenyl-hydrazone (CCCP) on intracytoplasmic membrane (ICM) assembly was examined in the purple bacterium *Rhodobacter sphaeroides*. CCCP blocks generation of the electrochemical proton gradient required for integral membrane protein insertion. ICM formation was induced for 8 h, followed by a 4-h exposure to CCCP. Measurements of fluorescence induction/relaxation kinetics showed that CCCP caused a diminished quantum yield, a cessation in expansion of the functional absorption cross-section and a 4- to 10-fold slowing in the electron transfer turnover rate. ICM vesicles (chromatophores) and an upper-pigmented band (UPB) containing ICM growth initiation sites, were isolated and subjected to clear-native electrophoresis. Proteomic analysis of the chromatophore gel bands indicated that CCCP produced a 2.7-fold reduction in spectral counts in the preferentially assembled light-harvesting 2 (LH2) antenna, while the RC-LH1 complex, F_1F_O-ATPase and pyridine nucleotide transhydrogenase decreased by 1.7–1.9-fold. For 35 soluble enzymes, the ratio of 0.99 for treated/control proteins demonstrated that protein synthesis was unaffected by CCCP, suggesting that the membrane complex decline arose from the turnover of unassembled apoproteins. In the UPB fraction, an ~2-fold accumulation was observed for the preprotein translocase SecY, the SecA translocation ATPase, SecD and SecF insertion components, and chaperonins DnaJ and DnaK, consistent with the possibility that these factors, which act early in the assembly process, have accumulated in association with nascent polypeptides as stabilized assembly intermediates.

© 2015 Elsevier B.V. All rights reserved.

1. Introduction

Rhodobacter sphaeroides is a purple chlorophototrophic Proteobacterium of the α-3 subclass that provides a unique combination of extensive metabolic capabilities and accessible molecular genetics with an intracytoplasmic membrane (ICM) amenable to an unparalleled variety of biochemical, spectroscopic, and ultrastructural probes. Accordingly, this system provides an ideal experimental model for examining the development and assembly of energy transducing membranes [1–5]. An ICM housing the photosynthetic apparatus is formed under both anoxic conditions in the light and at reduced oxygen tension in the dark. Atomic force microscopy (AFM) topographs obtained at submolecular resolution have shown that the ICM of *Rba. sphaeroides* consists of rows of dimeric reaction center-light-harvesting 1 (RC-LH1) core complexes interspersed with narrow lanes of the peripheral LH2 antenna. At low illumination levels, the LH2 complex also forms LH2-only domains [1,5] that comprise the light-responsive antenna complement. Radiant energy harvested by LH2 is transferred to LH1, which funnels these excitations to the RC-bacteriochlorophyll *a* (BChl) special pair where they are transduced into a transmembrane charge separation. This initiates a cycle of electron transfer reactions between the primary iron-quinone acceptor (Q_A), the secondary quinone (Q_B), the ubiquinone pool, the ubiquinol-cytochrome c_2 oxidoreductase (cytochrome bc_1 complex), cytochrome c_2 and the photooxidized special pair, resulting in the generation of an electrochemical proton gradient that is coupled to the synthesis of ATP [1].

Recently, *Rba. sphaeroides* has also been established as a unique paradigm for structural and functional proteomic analyses of the ICM assembly process, insofar as the key components of the relevant proteome can be temporally expressed and spatially localized within the internal membrane structure of the cell [6,7]. The temporal expression of the key protein complexes and factors essential for their assembly

Abbreviations: AFM, atomic force microscopy; BChl, bacteriochlorophyll *a*; β-OG, *n*-octyl β-D-glucopyranoside; CCCP, carbonyl-cyanide m-chlorophenyl-hydrazone; CM, cytoplasmic membrane; CNE, clear native electrophoresis; COGs, clusters of orthologous groups; DOC, deoxycholate; FIRe, Fluorescence Induction and Relaxation; F_M, maximal fluorescence; F_V, variable fluorescence; F_V/F_M, the quantum yield of the primary charge separation; ICM, intracytoplasmic membrane; LH, light harvesting; LH1, core light-harvesting complex; LH2, peripheral light-harvesting complex; Q_A, primary reaction center ubiquinone; Q_B, secondary reaction center ubiquinone; RC, photochemical reaction center; σ, functional absorption cross-section; τ_{ET}, the rate of RC electron transfer turnover; UPB, upper pigmented band containing ICM growth initiation sites

* Corresponding author.
E-mail address: rniederm@rci.rutgers.edu (R.A. Niederman).

http://dx.doi.org/10.1016/j.bbabio.2015.06.002
0005-2728/© 2015 Elsevier B.V. All rights reserved.

within the developing membrane template can be readily controlled in cells undergoing both adaptation to reduced light intensity [7–10] and gratuitous induction of ICM formation (greening) when cells are transferred from high to low oxygen tension [3,9]. Moreover, the membrane development process can be spatially localized to both invaginating cytoplasmic membrane (CM) and mature ICM vesicles, which give rise to respective upper-pigmented band (UPB) and chromatophore band during rate-zone sedimentation on sucrose density gradients [4,11]. This facilitates assessment of the proteomes arising from distinct membrane regions at various stages of ICM development.

In the present study, we have examined the effects of the lipid-soluble protonophore carbonyl-cyanide m-chlorophenylhydrazone (CCCP) on the induction of ICM formation under low aeration in concentrated cell suspensions. CCCP serves as a potent uncoupler of electron transfer from ATP synthesis [12] by blocking formation of the electrochemical proton gradient generated during electron transport by the respiratory chain carriers [13]. Integration of CCCP into the CM in an anionic form results in proton acquisition from the periplasmic space. After diffusion of the protonated CCCP form across the bilayer, protons are discharged into the cytoplasm, leading to collapse of the electrochemical proton gradient and leaving CCCP in the anionic state. Multiple repetitions of this process ultimately serve to short-circuit the respiratory chain.

In the closely-related purple bacterium *Rodobacter capsulatus*, CCCP concentrations sufficient to block cytochrome c_2 export to the periplasmic space, were shown to abolish the integration of the LH2-α polypeptide subunit into the ICM for entry into LH2 complex formation [14]. This suggested that the maintenance of an electrochemical proton gradient is essential for membrane translocation of such pigment-binding proteins. An order for integral LH protein assembly events was delineated, in which the chaperonin-assisted nascent proteins first bind to the cytoplasmic face of the ICM, undergo proton-motive force dependent ICM insertion to assume a transmembrane orientation, that is appropriate for pigment binding and assembly into functional complexes to subsequently occur. Using a membrane coupled cell-free translation system developed for studying LH1 assembly in *Rba. capsulatus*, depletion of the chaperonin DnaK significantly reduced the rate of synthesis and membrane insertion of both the LH1-α and -β polypeptides. Removal of the GroEL chaperonin from the *in vitro* translation system affected stable LH1 insertion into the coupled membranes, which was also dependent on the presence of unknown, membrane-bound factors [15,16].

Disrupting photosystem assembly in the cyanobacterium *Synechocystis* 6803 has been used as a strategy for the accumulation of distinct transient assembly intermediates [17]. This formed the basis for the elucidation of protein factors involved in photosystem (PS) biogenesis, which lead to the identification of Psb28, important for chlorophyll (Chl) biosynthesis as well as for formation of the apoprotein subunits of Chl-binding proteins [18]. These included the CP47 PSII antenna complex and PSI RC core proteins PsaA and PsaB. Subsequently, the Psb27 assembly factor has been shown to associate with the unassembled CP43 PSII antenna complex, with larger CP43 containing complexes, as well as the PsaB core protein of PSI [19]. Associations between this factor and components involved in the assembly process to form transient assembly intermediates were demonstrated by comigration in native electrophoresis, co-purification with His-tagged PSI and a yeast two-hybrid assay. The assembly of energy transducing complexes in the ICM of purple bacteria has recently been reviewed [20–22] and the need for a more complete understanding of this process has been emphasized. Moreover, identification of transient assembly intermediates as in cyanobacteria would be of considerable interest toward meeting this goal.

For the present work, chromatophores and the UPB fractions were isolated from *Rba. sphaeroides* cells in which CCCP was added during the induction of ICM formation, to block generation of the electrochemical proton gradient necessary for insertion of energy-transducing proteins into the membrane. These membrane fractions, in parallel with those isolated from an untreated control culture, were subjected to clear-native electrophoresis (CNE) to resolve their pigment-protein complexes for proteomic analysis. This has provided a critical test of the possibility that partially assembled complexes can be isolated from the CCCP-treated cells in a form in which transient associations with participating assembly factors are retained.

2. Materials and methods

2.1. Cell growth, ICM induction, and membrane isolation

ICM formation was induced in low-aeration suspensions of *Rba. sphaeroides* strain NCIB8253 essentially as described previously [3]. Cells grown chemoheterotrophically at 30 °C under high aeration (300 rpm on a gyratory shaker in the dark) into the logarithmic phase were harvested by centrifugation at 10,000 × *g* and 4 °C, resuspended in fresh medium to an $OD_{680\ nm} \approx 2.0$ (light path = 10 mm), divided into two 400-ml aliquots in 500-ml Erlenmeyer flasks and incubated under semiaerobic conditions by lowering the shaking rate to 200 rpm. After 8 h, 400 μl of 50 mM CCCP in DMSO was added to one culture (50 μM, final concentration), while DMSO alone was added to the control culture. After four h of additional incubation, both cultures were harvested for membrane isolation, performed in 1 mM Tris, pH 7.5, at 4 °C. The cells were centrifuged at 12,000 *g*, washed and a few crystals of DNAseI and protease inhibitor cocktail (both obtained from Roche) were added to the resuspended cell pellets, which were passed twice through a French pressure cell. Debris and unbroken cells were removed by centrifugation at 16,000 × *g*. The supernatant was layered onto a 5–35% (w/w) sucrose gradient prepared over a 60% (w/w) sucrose cushion and subjected to rate-zone ultracentrifugation for 3 h at 28,000 rpm in Beckman SW-28 rotor. Two pigmented bands were resolved: the UPB, containing membrane growth initiation sites and the ICM-derived chromatophore vesicles, which formed a broad pigmented band centered just below the middle of the gradient. Comigrating ribosomal and soluble material was separated from the membrane components of the UPB fraction by aqueous partitioning in a two-phase dextran–polyethylene glycol system as described previously [7]. Protein concentrations of membrane samples were determined using the bicinchoninic acid assay procedure (Thermo Scientific) with bovine serum albumin as standard.

2.2. Clear-native electrophoresis

Chromatophore fractions were solubilized with *n*-octyl β-D-glucopyranoside (β-OG) and deoxycholate (DOC) at concentrations of 15 mM each and subjected to CNE as described by Wittig et al. [23]. For CNE of the UPB fraction, solubilization was performed with digitonin (2 g digitonin/g total protein). Solubilized membrane samples were applied to polyacrylamide gradient gels and subjected to electrophoresis at 4 °C in a Vertical Slab Unit Model SE-400 (Hoeffer Scientific Instruments) at a constant current of 10 mA, until current was no longer measurable (~6 h). Unstained gels were scanned with a Canon visible light scanner, allowing visualization of up to four pigmented bands. They were quantified by scanning in a Typhoon imager (GE Healthcare) set in the fluorescence mode with a blue laser excitation source (488 nm) and a 670-nm emission filter; a plastic transparency was placed on top of the gel to provide uniform background fluorescence, such that the pigmented proteins appeared as white bands. Pigment-protein complex composition of excised gel bands was determined directly from absorption spectra obtained with a Beckman DU-640 spectrophotometer, using an excised gel slice, lacking sample as a blank. Gels for proteomic analysis were stained with Coomassie blue G250 (GelCode blue safe protein stain, Thermo).

2.3. Proteomic analysis

Gel bands resolved in CNE were excised, fixed for at least 30 min in 40% methanol, 10% acetic acid and subjected to in-gel digestion with trypsin, followed by LC-MS/MS using a Dionex U-3000 nanoflow liquid chromatography system in line with a Thermo LTQ linear ion trap mass spectrometer, operated in the nanoLC mode to obtain sub-femtomol sensitivity. For MS/MS a 135-min gradient was used for analysis of the gel bands of the whole UPB samples, while for pigmented bands from CNE, a 50-min gradient was employed. Database analysis of peaks generated from LTQ data was performed as described by Sleat et al. [24] in which tandem mass spectrometry data files were searched against the NCBI assembly of the annotated *Rba. sphaeroides* 2.4.1 genome [25]. Proteomics data were quantified by spectral counting, which measures protein abundance on the basis of the number of tandem mass spectral observation for all constituent peptides. Spectral count sampling statistics have high technical reproducibility and therefore can be successfully applied for assessment of relative protein abundance and differential protein expression studies in mass label-free LC-MS/MS [6,26]. While label-free approaches have wider dynamic range and broader proteome coverage, stable isotope labeling offers higher quantification precision and accuracy. Fragment mass tolerance was 0.4 Da with a cutoff of the log of the expectation score = <−5, and at least two unique peptides. The exact binomial test was used to determine whether ratios were significantly different, while p values were transformed to q values to control the false discovery rate among multiple comparisons. The list of pairwise comparisons was filtered to exclude the proteins with combined spectral counts <5, and their assignments as noted in the text, were considered as tentative.

2.4. Fluorescence Induction/Relaxation measurements

Fluorescence Induction/Relaxation (FIRe) transients of inducing *Rba. sphaeroides* cell preparations were measured in a Fluorescence Induction and Relaxation system (Satlantic Inc., Halifax, Nova Scotia). Measurements were made on whole cells diluted typically to ~30 nM BChl in growth medium to produce transients in the linear range. A blue LED (450 nm, 30-nm bandwidth) serves as the excitation source, which is controlled by an LED circuit driver capable of generating pulses of 1 ms to 50 ms duration. Fluorescence emission is passed through an 880-nm interference filter (50-nm bandwidth) and detected by a sensitive avalanche photodiode module. The digitized fluorescence kinetic transients obtained at 880 nm are processed by computer-assisted analysis, which translates measured signals to programmed physiological parameters, following a charge separation elicited between the RC-BChl special pair and Q_A. These parameters form the basis for the functional analysis described here. F_V/F_M and σ are extracted from the initial rapid phase of the fluorescence induction curve [3,8], where σ is calculated from the slope of the single turnover saturation curve and is related to the rate of increase in fluorescence yield. Since it was not known to what extent the relaxation kinetics reflected RC-BChl special pair re-reduction or Q_A re-oxidation, the multiphasic relaxation profile is expressed as the RC electron transfer turnover rate, designated as τ_{ET}. A recent study [27] has suggested a role for the soluble cytochrome c_2 periplasmic diffusion pathway between the cytochrome bc_1 complex and the RC in accounting for the fluorescence relaxation kinetics.

In previous studies [3,8,9], values obtained for the functional absorption cross-section, reflecting the functional antennae size, ranged from 28 to 130 Å^2, roughly corresponding to ~32–155 BChl per RC. The functional absorption cross-section is expressed here as $\sigma_{450\ nm}$, the maximum wavelength of the blue LED excitation source, which excites LH1- and LH2-bound spheroidenone to the $S_2(1Bu^+)$ state, from which excitation energy is transferred to both the Q_X- and Q_Y-bands of the LH1 and LH2 BChls [28].

3. Results

3.1. Proteomic analysis of pigment-protein complexes separated by clear native electrophoresis

For CNE, chromatophores were solubilized with an *n*-octyl β-D-glucopyranoside/deoxycholate (β-OG/DOC, 1:1) mixture which results in the resolution of pigment-protein complexes into four distinct pigmented bands [7]. The respective top and bottom bands consisted of the RC-LH1 (B875) core and LH2 (B800-850) peripheral antenna complexes in a spectrally homogenous form. Two bands of intermediate migration, apparently reflecting native associations of the LH2 and core complexes were resolved; the upper intermediate band was enriched in LH2 (designated as the LH2-LH1 band) while the lower one was RC-LH1 enriched (LH1–LH2 band). These intermediate complexes are thought to represent detergent-protein micelles arising from ICM regions where the LH2 and LH1 complexes remain in contact as seen initially in AFM topographs obtained at submolecular resolution [29]. An analysis of electrophoretic migration behavior suggested that the upper intermediate LH2–LH1 band represents a $[RC\text{-}LH1][LH2]_2$ aggregate, while the lower LH1–LH2 intermediate band migrated as an aggregate of [RC-LH1][LH2] monomers [10]. The top band migrated as an $[RC\text{-}LH1]_2$ dimer, with the bottom band having the migration behavior of an $[LH2]_3$ trimer. The lower intermediate (LH1–LH2) band is thought to be derived from regions of the ICM in which LH2 associates at the outer edges of the rows of dimeric RC-LH1 core complexes observed in AFM. In contrast, the upper intermediate (LH2–LH1) band may arise from areas of LH2–LH1 associations found at narrow rows of LH2 rings situated between the linear arrays of dimeric LH1-RC core complexes [10].

It was necessary to resort to a gentler procedure employing the mild detergent digitonin in place of β-OG/DOC to resolve putative CM invagination sites within the UPB into discreet pigmented bands (Fig. 1). While digitonin-treated chromatophores were still resolved into four bands, the low LH2 content of the UPB resulted in the appearance of only the top band, lower intermediate band and a diminished LH2 bottom band. Like their chromatophore counterparts [7,10], the respective UPB top and bottom bands represented spectrally pure RC-LH1 and LH2 complexes while the lower intermediate band was again enriched in LH1 relative to LH2 (Fig. 1C). The UV absorbance profile of all three UPB bands suggested that nucleic acid and soluble protein contaminants had been largely removed from the UPB preparation.

In order to establish a baseline for protein components migrating in the CNE bands from the UPB, the UPB top (RC-LH1) and lower intermediate (LH1–LH2) bands were subjected to proteomic analysis and compared with their chromatophore counterparts (Fig. 2). These proteomic data are expressed in spectral counts and mainly reflect the ability of trypsin to act at potential cleavage sites and are therefore only semiquantitative in nature. Accordingly, proteins that are not highly abundant with a large number of accessible sites can give rise to higher counts than more abundant proteins with far fewer sites; in cases where no sites are available, no counts are found, *viz*., PufB (LH1-β-polypeptide) and PucA (LH2-α); however, the latter polypeptide could be detected after chymotrypsin cleavage [10]. Nevertheless, since the gel lanes were loaded with equal amounts of total protein, valid comparisons can be made between the same protein components in the chromatophore and UPB preparations and the designated clusters of orthologous groups (COGs) into which the proteins are classified [31].

The RC-LH1 complex accounted for the majority (52%) of spectral counts in the top (RC-LH1) band of chromatophores compared to less than a third (29%) for the UPB, demonstrating that the UPB band contains vastly more non-pigmented protein. In comparison to their equivalent chromatophore gel bands, both UPB bands were enriched in CM markers: *viz*., succinate dehydrogenase (~2–4-fold), other electron transfer enzymes (up to ~2-fold), transport proteins (3-fold), as well as general membrane assembly factors (up to 2-fold). These included

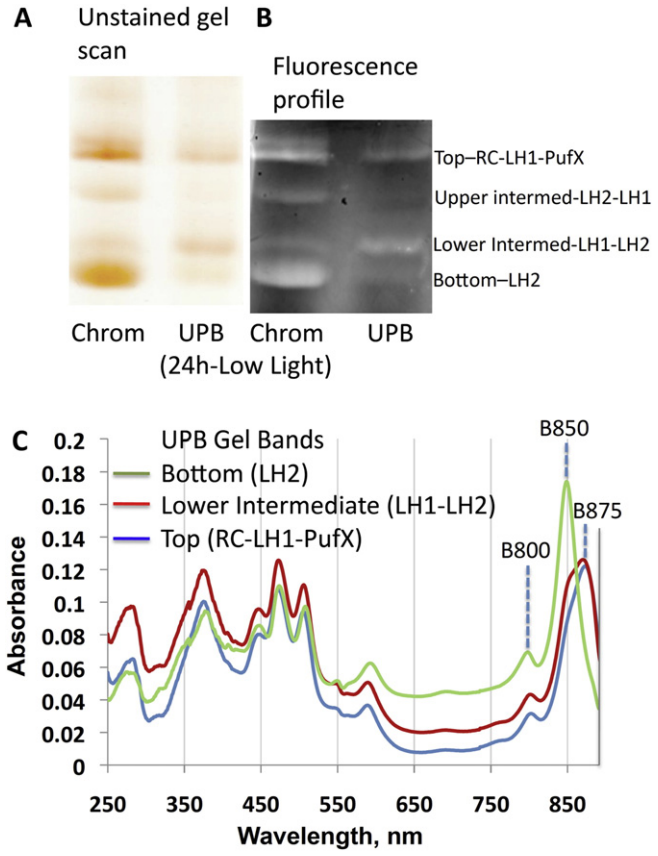

Fig. 1. Separation of intact pigment-protein complexes by CNE of digitonin-solubilized membrane fractions. Cells were subjected to a 24-h adaptation from high (1100 W/m^2) to low intensity illumination (100 W/m^2) [7]. UPB and chromatophore fractions were isolated by rate-zone sedimentation and UPB was further purified by a two-phase partitioning procedure [7]. The purified membrane preparations were solubilized with digitonin (2 g/g protein), applied to a gel slab formed with a 5–10% polyacrylamide gradient and subjected to CNE. A. Left, scan of unstained gel; B. image obtained with Typhoon scanner as described in Materials and Methods, pigmented proteins give rise to the white bands. C. Absorption spectra obtained directly on indicated UPB gel slices. The high level of spectral purity of the top (RC-LH1-PufX) band is indicated by the presence of the LH1 Q_y absorption band at 875 nm and the RC monomeric BChl band at 802 nm, and for the bottom (LH2) band by the maxima at 800 and 850, arising from the Q_y bands of the respective LH2 monomeric and dimeric BChl components. An LH1 enrichment is also seen in the lower intermediate (LH1–LH2) band. The differences in carotenoid content between the RC-LH1 core complex and LH2 reflects the respective BChl-carotenoid molar ratios near 1.0 for LH1 and ~2.0 for LH2 [30]. Note also the expected blueshift in the position of the red-most carotenoid absorption (0–0 vibrational) band in LH1 relative to LH2 (respective absorption maxima at 505 and 508 nm). The relatively low levels of UV absorbance indicate extensive purification of these complexes on a protein basis.

significant levels of the preprotein translocases YidC, YajC, and SecY, bacterial type 1 signal peptidase and twin arg translocation subunit TatA. Importantly, such general membrane assembly factors were significantly enriched in the UPB RC-LH1 gel bands, confirming the active role of membrane invagination sites in pigment-protein complex assembly. This overall profile of protein enrichment confirms that the UPB arises from both the peripheral respiratory CM and CM invagination sites [4], the latter serving as the hotspots for LH and RC complex assembly [33].

3.2. CCCP arrests synthesis of membrane protein complexes and slows light-driven cyclic electron flow during ICM induction

In an effort to determine whether CCCP-induced dissipation of the electrochemical proton gradient required for insertion of nascent LH apoproteins into the membrane results in the accumulation of early assembly factors in association with participating polypeptides undergoing membrane insertion, ICM formation was induced as follows. Concentrated suspensions of chemoheterotrophically grown cells, essentially devoid of BChl, were shifted to semiaerobic conditions by lowering the shaking rate as described in Experimental Procedures. Under these conditions, BChl synthesis is induced as reflected here by the gradual rise in the $OD_{850\ nm}/OD_{680\ nm}$ in the concentrated cell suspensions over the first 8 h of the induction process (Fig. 3A). This was characterized by an increase in the number of both the RC-LH1 core and peripheral LH2 antenna complexes, in which the preferential appearance of the core particles is followed by an accelerated accumulation of LH2 [3], as reflected in the >4-fold increase in the molar LH2/LH1 ratio over this time period (Fig. 3B). The small increase in $OD_{680\ nm}$ over the first eight h (~1.5 OD units) confirmed that only limited cell division had occurred in these concentrated cell suspensions and that functional changes largely reflected accelerated synthesis of pigments and their binding proteins in existing cells. Therefore, these resting cell preparations in which a sequential assembly of RC-LH1 and LH2 complexes is occurring, provide an ideal system for examining the effects of inhibition of the electrochemical proton gradient on the active assembly of pigment-protein complexes.

It can be seen that following CCCP addition at 8 h, a cessation in the appearance of pigment-protein complexes has occurred (Fig. 3B). This is shown most dramatically by the near-IR absorption spectra of the inducing cells (Fig. 3C) in which no further absorption attributable to the LH1 or LH2 is found at either 9 or 12 h. Determination of the effect of CCCP on the photosynthetic activities of the inducing cells by FIRe measurements showed a marked reduction in the quantum yield of the primary charge separation, as assessed from the F_V/F_M values (Fig. 4A). The functional absorption cross-section ($\sigma_{450\ nm}$), which more than doubled in the control culture from ~43 Å^2 at the outset to ~89 Å^2 at 12 h (Fig. 4B), leveled off after the first h of CCCP addition, reflecting the cessation in LH complex assembly in the presence of the inhibitor as shown in Fig. 3. A more dramatic effect of CCCP was observed on the rate of RC electron transfer turnover (τ_{ET}) (Fig. 4C). In contrast to the previously observed gradual diminution of τ_{ET} [3,7] as seen in the control culture, a >4-fold slowing, from 2.4 to 11.5 ms, occurred within the first hour after addition of the protonophore. It is important to stress that the multiple cycles of CCCP inhibition lead to a collapse of the proton gradient and to the short-circuiting of the respiratory chain. It might be possible that the short-circuiting of the electron transfer chain would affect donor side electron transfer, insofar as the short-circuit would be expected to occur at the proton release phases in the Q-cycle of the bc_1 complex. Significantly, the protonophore-based inhibition of these physiological parameters as shown by FIRe analysis, suggests that 50 μM CCCP should be more than sufficient to block the membrane-potential requiring insertion of nascent polypeptide chains into the membrane bilayer, a possibility that is further explored in the proteomic investigation described below.

3.3. Proteomic analysis of membrane fractions isolated from CCCP-inhibited cells undergoing ICM induction

Chromatophore and UPB fractions were isolated from CCCP-treated and untreated control cells and subjected to CNE for proteomic analysis of the resulting gel bands. Four pigmented bands were present after CNE, as observed for chromatophores from the cells undergoing adaptation to low light intensity (Fig. 1). Because these gel bands were expected to contain membrane protein assembly factors (Fig. 2), this native electrophoresis procedure provided the basis for a critical proteomic analysis of light-harvesting, reaction center and other integral membrane protein assembly processes.

Supplementary Figs. S1 and S2 indicate that the gel bands arising from the chromatophore preparations from the inducing cells also gave rise to a large number of proteins when subjected to LC-MS/MS. Fig. 5 shows the effects of CCCP treatment on the LH, RC, and related energy transduction complexes from the major bands. CCCP markedly

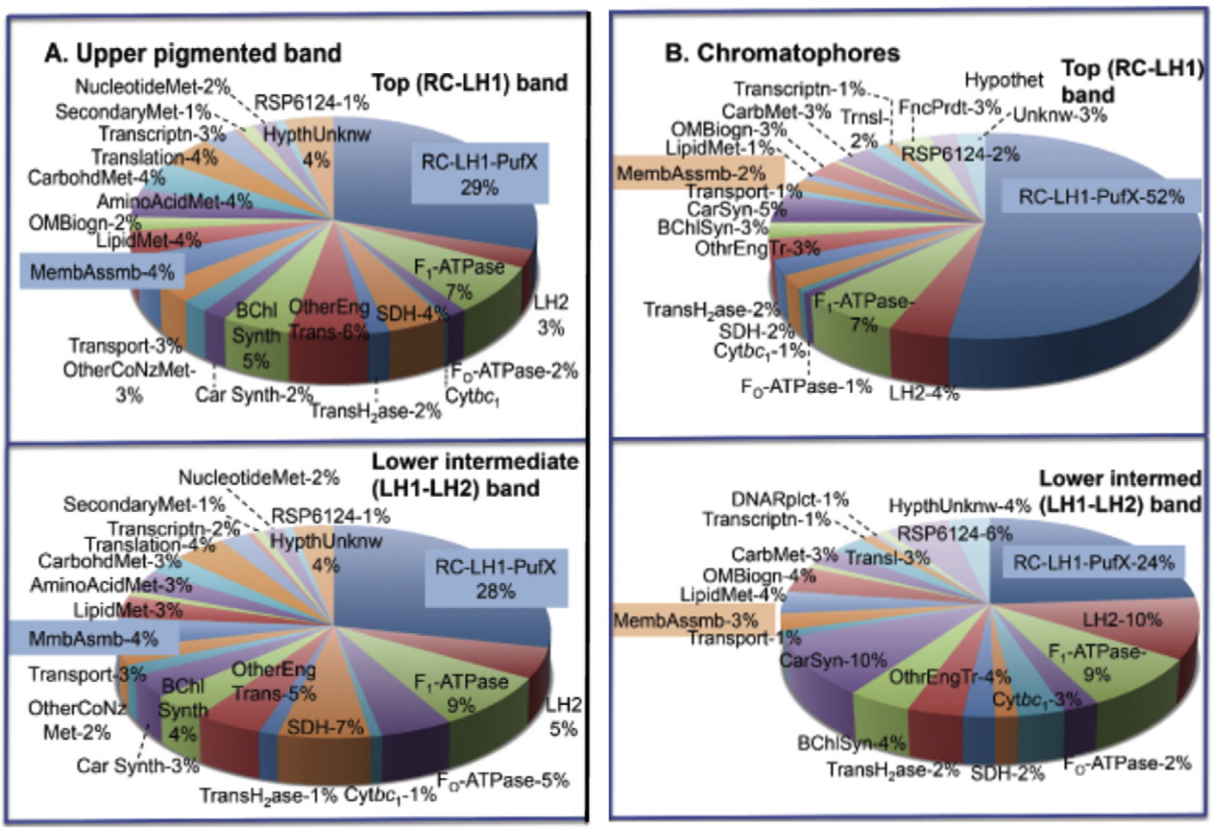

Fig. 2. Proteomic analysis of UPB (A) and chromatophore (B) CNE gel bands. Membrane fractions were isolated from cells after a 24-h adaptation to a light intensity of 100 W/m^2 [7]; the UPB and chromatophores were solubilized with digitonin and β-OG/DOC, respectively, and the resolved CNE bands shown in Fig. 1 were subjected to in-gel trypsin digestion and LC-MS/MS as described in Materials and Methods. The distributions shown are for clusters of orthologous groups (COGS) [31], in which the usual energy production and conversion category has been divided into subgroups to account for the distinct metabolic capabilities unique to photoheterotrophically growing *Rba. sphaeroides* [7].

blocked membrane insertion of polypeptides of the LH2, RC-LH1, and F_1F_O-ATPase complexes, especially in the respective gel bands in which they were found in the highest levels (Fig. S2). Accordingly, for the LH2 complex in the bottom (LH2) band, a 2.7-fold reduction in spectral counts was observed, consistent with the accelerated rate of LH2 synthesis and assembly at this stage of the induction process (Fig. 3B). A 1.7-fold reduction was found for the RC-LH1 complex in the top (RC-LH1) band and 1.9- and 1.8-fold reductions in the upper intermediate band for the F_1-ATPase and F_O-ATPase, respectively. The pyridine nucleotide transhydrogenase, an additional energy transducing ICM-associated protein complex, showed a CCCP-induced spectral count reduction of 1.7-fold, averaged over all four gel bands. Thus, this complex, along with the RC-LH1 core and F_1F_O-ATPase complexes, with spectral count decreases in the of 1.7–1.9-fold range, reflect the interruption by CCCP of the membrane insertion of complexes with rates of assembly at a basal level during this stage of ICM induction, rather than at the accelerated rate seen for the LH2 complex. In addition these results provide new *in vivo* evidence confirming that the maintenance of an electrochemical proton gradient is essential for membrane translocation of the integral LH2 apoproteins [14] and extends these findings to the RC-LH1, transhydrogenase and F_1F_O-ATPase complexes.

Fig. 5 also shows the levels of spectral counts for 35 soluble proteins representing enzymes of amino acid and carbohydrate metabolism. The ratio of 0.99 for the CCCP-treated *vs.* control proteins demonstrated that the synthesis of soluble proteins was unaffected by protonophore treatment. This suggests that the CCCP-induced major decline in levels of the energy-transducing membrane protein complexes shown in Fig. 5 can be attributed to a blockage in the electrochemical protein gradient necessary for their membrane insertion rather than a CCCP-induced general arrest in protein biosynthesis. Instead, it is expected that the synthesized membrane proteins, in the absence of the electrochemical proton gradient needed for their membrane insertion, undergo accelerated turnover rather than insertion into the ICM as blocked by CCCP. A significant reduction in spectral counts was also induced by CCCP in enzymes of BChl and carotenoid synthesis (1.6- and 1.7-fold, respectively) (Figs. S1 and S2). While the majority of these enzymes represent soluble proteins, it is possible that they are degraded in the absence of appropriate associations with membrane components required for the coordination of their respective pathways of pigment biosynthesis with concomitant formation of pigment binding apoproteins of the LH and RC complexes.

The effect of CCCP treatment on the proteomic profile of several clusters of orthologous groups in the overall UPB fractions is shown in Figs. 6 and S3. Of most significance is the CCCP-induced increase in levels of general membrane assembly factors (Fig. 6A) for which the effects on the individual factors are shown in Fig. 6B and C. This can be largely accounted for by the ~2-fold greater accumulation of the preprotein translocase SecY, the SecA translocation ATPase, SecD and SecF insertion components, and chaperonins DnaJ and DnaK. We suggest that these general membrane assembly factors have accumulated largely in association with nascent polypeptides in the form of assembly intermediates of the photosynthetic and energy-transducing complexes that have failed to dissociate under the inhibitory conditions. In comparison to control levels, SPFH, Ftsh, and HflC were also elevated in the presence of CCCP, which is discussed further below. It is tempting to speculate that the accumulated assembly factors represent intermediates in the assembly process in which nascent proteins remain associated, in a form in which these intermediates are protected from proteolytic degradation.

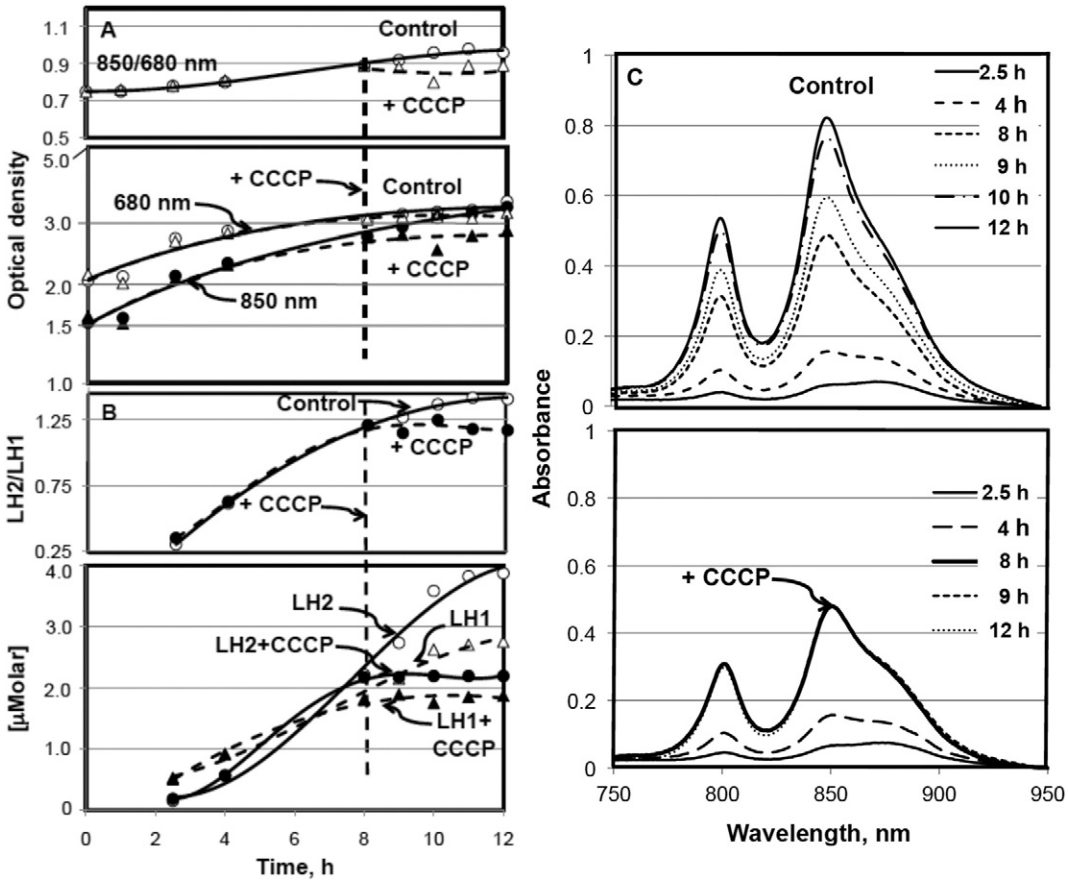

Fig. 3. Induction of ICM formation in low-aeration cell suspensions. A. Top panel: $OD_{850/680\ nm}$ ratio where $OD_{680\ nm}$ represents cell density determined at a wavelength devoid of pigment absorption bands, while OD_{850} arises from the redmost Q_Y-absorption bands of the LH complexes superimposed on the intrinsic cell light scattering. At 8 h, CCCP was added to one culture to a final concentration of 50 μM, and after 4 h of additional incubation, both the CCCP-treated and control cultures were harvested for preparation of French-press extracts and membrane isolation as described in Materials and Methods. Bottom panel: kinetics of cell optical density ($OD_{680\ nm}$) increase and accumulation of LH complexes (OD_{850}) B. Top panel: Molar ratios of LH2/LH1 determined with established molar extinction coefficients after correcting for light scattering and deconvolution of near-IR absorption spectra [32]. Bottom panel: Differential synthesis of LH2 and LH1 complexes. C. Near-IR absorption spectra of whole inducing cells after correction for light scattering; the Q_Y-absorption band of the LH1 core antenna complex has a maximum at 875 nm (B875 band) as seen in the 2.5 and 4 h spectra, while the Q_Y-absorption bands of the LH2 peripheral antenna complex has maxima at 800 and 850 nm (B800 and B850 bands), most evident in the 12 h control spectrum.

4. Discussion

This study has been facilitated by development of a non-denaturing polyacrylamide gel electrophoresis procedure for the isolation of native LH2 and RC-LH1 complexes for proteomic analysis [7]. The initial procedure employing membrane solubilization with a β-OG/DOC mixture was successful in facilitating CNE with chromatophores, but it was necessary to resort to the milder detergent solubilization conditions provided by digitonin to satisfactorily resolve these complexes from the UPB. While their absorbance spectra demonstrated a high level of spectral purity for the RC-LH1 upper and the LH2 lower bands, proteomic analysis showed significant spectral counts arising from a variety of other proteins, the majority of which were integral to the chromatophore and UPB membranes. Since labile protein–protein interactions are expected to be preserved after digitonin solubilization [23], it is tempting to speculate that the high spectral counts for at least some of these integral membrane proteins may represent supramolecular associations with the LH2 and RC-LH1 complex in the form of multi-protein complexes. As a consequence of the tightly packed LH2 and RC-LH1 domains observed in AFM topographs [29,34], intercomplex associations would be expected to occur at the edges of these extensive arrays.

Further support for such intercomplex organization comes from a recent study of energy and electron transfer integration in the *Rba. sphaeroides* ICM [35]. In AFM topographs, His-tagged, dimeric cytochrome bc_1 complexes labeled with gold nanobeads appeared mainly in the region of RC-LH1 core complexes. Moreover, after partial detergent solubilization of chromatophores, the cytochrome bc_1 and RC-LH1 complexes co-purified, while LH2 complexes were detached. This appeared to reflect the observed clusters of cytochrome bc_1 complexes in association with RC-LH1 arrays, but not in fixed stoichiometric bc_1-RC-LH1-supercomplexes [36]. Instead, bc_1 complexes are seen adjacent to RC-LH1 complexes in disordered areas leaving the majority of the RC-LH1 complexes out of contact with cytochrome bc_1.

A detailed proteomic analysis of *Rba. sphaeroides* membranes has recently been reported [37] in which 43 unique proteins were identified in the highly specialized chromatophore membrane as compared to 236 making up the more complex membrane components isolated in the UPB fraction. A meatabolically stable isotope labeling procedure permitted determination of the relative distribution of proteins between the chromatophores and the UPB, revealing that the UPB is enriched in enzymes of lipid and tetrapyrrole biosynthesis. In contrast, the chromatophore fraction had higher levels of LH and RC proteins as well as the cytochrome bc_1 complex, the F_1F_O-ATPase and transhydrogenase. This suggested that a spatial proximity of the photon collecting and energy transduction machinery exists within the ICM, in which light energy is ultimately conserved by production of ATP. The results of this stable isotope labeling of the UPB and chromatophore fractions [37] also supported mechanisms established in *Escherichia coli* for the assembly of the F_1F_O-ATPase [38] and transhydrogenase [39] complexes. These proteomic data demonstrated the existence in the UPB of F_1F_O-

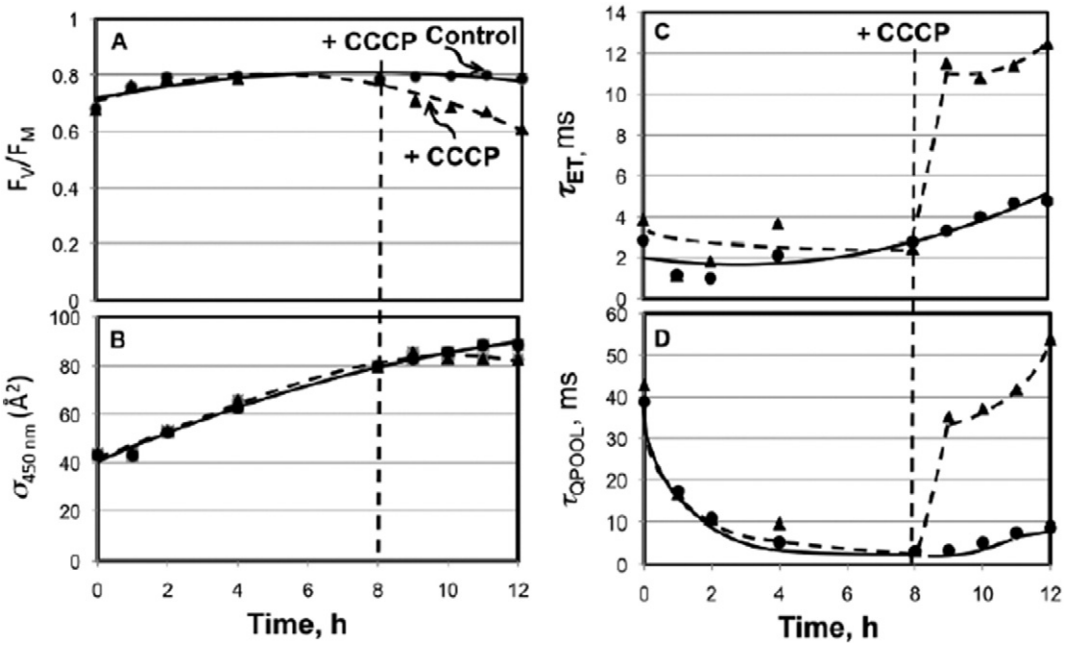

Fig. 4. Effect of CCCP on functional parameters of cells undergoing ICM induction. Determined from analysis of kinetic transient obtained by the FIRe analysis as described in Materials and Methods. Analyzed transients represented signal-averaged sets of 20 traces per sample, which minimized noise levels in individual traces. A, Quantum yield of primary charge separation (F_V/F_M) *vs.* induction time. B, Functional absorption cross-sections ($\sigma_{450\ nm}$) *vs.* induction time. C. Reaction center electron transfer turnover rates (τ_{QA}) *vs.* induction time. D. UQ pool re-oxidation ($\tau_{Q\ pool}$) *vs.* induction time. Lines through data points represent polynomial fits.

ATPase populations at various stages of the assembly process and provided evidence for post-insertional formation of the F_O subunit b_2 dimer prior to F_1 sector binding to the peripheral F_O-b_2 subunit stalk [38].

It is particularly noteworthy that our proteomic analyses revealed enrichment in a variety of general membrane assembly factors in the RC-LH1 gel band of the UPB relative to their levels in the same band from chromatophores. This suggests that these components could play roles in membrane insertion of the predominating LH1 and RC apoproteins during their preferential assembly in the UPB membranes

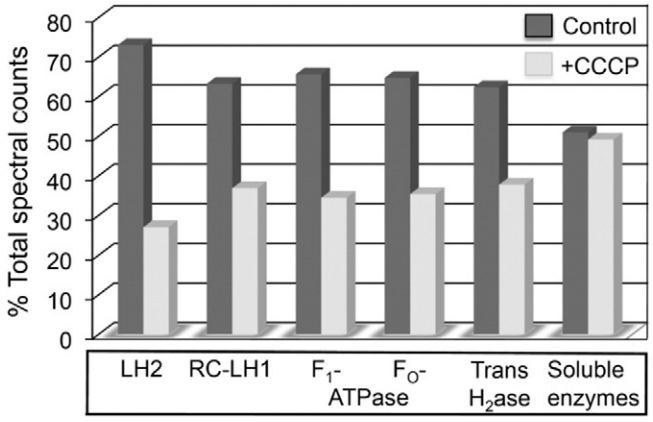

Fig. 5. Proteomic analysis of CNE gel bands from chromatophores isolated from CCCP-treated cells undergoing ICM induction. Details of CCCP treatment and chromatophore isolation by rate-zone sedimentation are described in Experimental Procedures. Chromatophores were solubilized with β-OG/DOC, gel bands were resolved by CNE and subjected to in-gel trypsin digestion and LC-MS/MS as described in Materials and Methods. The full COG distributions, including both membrane-associated and soluble proteins, for all four chromatophore gel bands are presented in Supplementary Fig. S1, while the effect of CCCP on individual components of interest within all four gel bands is shown in Supplementary Fig. S2.

arising from CM invagination sites that serve as hotspots for RC-LH1 core complex assembly [33,34]. These assembly factors included the twin arg translocation subunit TatA involved in translocation of the folded C-terminal domain of the Rieske Fe–S protein [40], the SecY component of the Sec YEG translocase, bacterial type 1 signal peptidase, as well as the YidC and YajC preprotein translocases. The Sec translocase is comprised of the integral membrane SecYEG polypeptides, which form a heterooligomeric channel [41] and the peripheral SecA translocation ATPase, thought to be essential in translocation of the large loops of integral membrane proteins. The YidC preprotein translocase functions as a membrane chaperonin, facilitating Sec translocase-dependent and -independent lateral bilayer movement [42]. For the former, YidC has been shown to bind to the SecY lateral gate and is detached in the presence of nascent membrane proteins, thereby facilitating their lipid bilayer transfer [43]. Yid C has also been demonstrated to possess a role in nascent protein folding and helix–helix interactions as part of the SecYEG machinery [44]. In addition, the Sec translocase-independent YidC driven pathway is strictly required in *E. coli* for membrane integration of the subunits a and c of the F_O sector of the F_1F_O ATPase [45] and Subunit II (CyoA) of the cytochrome *o* complex [46], which is driven by the electrochemical proton gradient. YidC is also bound directly to the SecDFYajC accessory complex [47], which links the Sec translocase complex to YidC, while SecD and SecF can participate in SecY independent insertion of proteins into the bilayer. In addition, a SecYEG–SecDF-YajC–YidC holo-translocon has been shown to be effectively involved in both the co-translational membrane protein insertion and posttranslational secretion processes [48].

Significantly, proteomic analysis of the overall UPB fraction showed that CCCP treatment resulted in accumulation of ~2-fold greater levels of a number of general membrane assembly factors (Fig. 6). These included the SecY preprotein translocase, the SecA translocation ATPase, SecD and SecF insertion components, as well as chaperonins DnaJ and tentatively DnaK, all of which are involved in early stages of the insertion of integral membrane proteins into the membrane bilayer. This suggested the possibility that these factors had accumulated in stable association with nascent polypeptide components as assembly

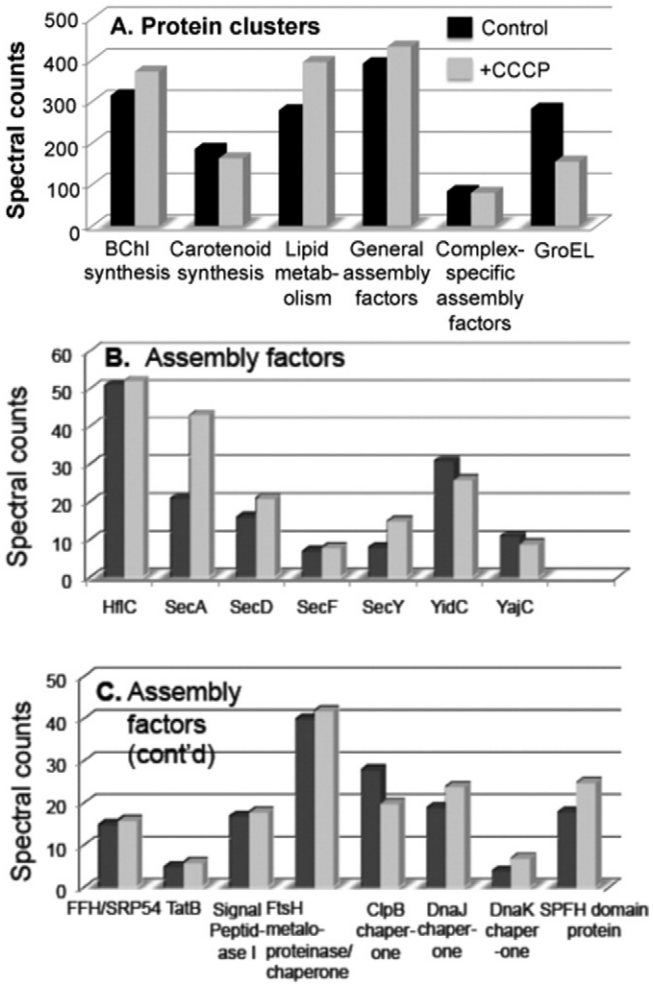

Fig. 6. Proteomic analysis of UPB fraction isolated from CCCP-treated cell suspensions undergoing ICM induction showing effects of CCCP on relevant protein clusters (A) and general membrane assembly factors (B, C). Details of CCCP treatment and UPB isolation by rate-zone sedimentation are described in Materials and Methods. Following removal from sucrose gradients, the UPB fraction was subjected to sodium dodecyl sulfate-polyacrylamide gel electrophoresis. After entering gel, bands were excised for in-gel trypsin digestion followed by LC-MS/MS in which a 135-min LC gradient was used for optimal peptide resolution. The full COG distributions, including both membrane-associated and soluble proteins from the UPB fractions of the CCCP-treated and -untreated control cell suspensions are presented in Supplementary Fig. S3.

intermediates that were not readily dissociated or degraded. Moreover, their accumulation can be attributed to a requirement for an electrochemical proton gradient for stable membrane protein insertion, which is inhibited when CCCP, by virtue of its lipid solubility, has integrated into the lipid bilayer. Further support for the possible accumulation of early stage assembly intermediates is the CCCP-induced decline in the levels of YidC and YagC, which have roles in later stages of the Sec translocase dependent prokaryotic membrane protein assembly process [47] and appear to have undergone degradation during CCCP treatment. The accumulation of the putative assembly intermediates would be expected to arise during the first and second stage of the proposed pathway for LH protein assembly [14]. These putative steps consist of the chaperonin-assisted binding of the nascent protein to the cytoplasmic face of the membrane, followed by their electrochemical proton gradient dependent ICM insertion before undergoing pigment binding and final assembly into functional complexes. Our results can also be reconciled with the lack of CCCP-induced accumulation of complex specific assembly factors (Fig. S3), having roles in late stage cofactor binding and assembly steps. Among these components with the highest spectral counts were the cytochrome *c*-type biogenesis protein, cycH [49], iron–sulfur cluster-binding protein [40] and LH1 assembly factors [50], all of which showed essentially no changes in levels in the UPB after CCCP treatment.

The FtsH metaloproteinase also remained slightly elevated during CCCP treatment (Fig. 6). This component functions as a membrane protease and chaperonin [51] and has been shown to cross-link with YidC and HflK/C, suggesting that these proteins play a linked role in the quality control of bacterial cytoplasmic membrane protein integration [52]. HflC, which functions along with HflK as a modulator of FtsH activity, and was also slightly elevated by CCCP treatment. HflK/C are members of the highly conserved SPFH domain proteins [53], and together they were considerably elevated in the UPB for the CCCP treated cells. Other components involved in early aspects of the membrane protein assembly that were also slightly elevated by CCCP included the signal recognition particle homologue Ffh/SRP54 [54] and signal peptidase I [55].

The recent AFM observation of "captive" proteins seen in association with LH1 rings formed in a RC-*Rba. sphaeroides* strain [56], provides *in vivo* structural support for the existence of membrane protein-assembly factor intermediates as suggested here from the proteomic analysis of CCCP-treated cells. The apparent presence of complete LH1 rings still associated with their assembly factors is thought to reflect the absence of an RC template, leading to LH1 formation around other proteins of appropriate dimensions. Integral membrane proteins of sufficient size to serve in this capacity include: (i) BChl synthase (BchG), involved in bacteriochlorophyllide esterification; (ii) LhaA, a RC-LH1 core assembly factor belonging to the major facilitator superfamily, forming part of the putative "BChl delivery branch" [50].

Proteomic analysis of the resolved CNE gel bands from the chromatophore fraction of the CCCP-treated cells also revealed that the spectral counts for the chaperonin GroEL were elevated relative to those in the untreated control preparation. This was most pronounced in the RC-LH1 band, accounting for 19 and 8% of the total, respectively, as well as in the upper intermediate (LH2–LH1) band (11% in CCCP treated-cells and negligible counts in control) (Fig. S1D, C). While in the CCCP-treated cells, this may also be a reflection of assembly intermediate accumulation, insofar as GroEL apparently serves as a chaperonin that catalyzes the appropriate folding of LH1-α and -β polypeptides for stable assembly into LH1 complexes [15,16], significant levels of the 29.9 kDa universal stress protein UspA were also found. UspA is a serine/threonine phosphoprotein that undergoes autophosphorylation in response to arrested growth [57]. UspA is expressed under conditions of challenged viability including starvation for nutrients, heat shock, DNA damage and osmotic and oxidative stress [58]. While the low aeration cells used here serve as a useful system to study the induction of ICM formation and assembly of the photosynthetic apparatus [3], only limited cell division occurs in these concentrated cell preparations (generation time of >12 h *vs.* ~3 h for phototrophically grown cells). Accordingly, expression of UspA indicates that the cells are also undergoing a stress response in which high levels of GroEL are formed to serve as a heat shock protein. Such elevated levels of GroEL assist in the folding of nascent proteins while also counteracting stress-induced protein denaturation by maintaining pre-existing proteins in stable conformations to prevent their aggregation on exposure to stress [59].

Supplementary data to this article can be found online at http://dx.doi.org/10.1016/j.bbabio.2015.06.002.

Author contributions

K. W. performed experiments, provided instruction and interpreted the data, O.B.O. and D.S. performed experiments, J.M.K. assisted in validation of the proteomics data, R.A.N. designed the experiments, interpreted the data and wrote the paper.

Conflict of interest

None of the authors have conflicts of interest associated with this study.

Acknowledgements

We thank Prof. Peter Lobel and Dr. Haiyan Zheng for conducting the proteomic analyses and assistance in data validation. Supported by grants to R.A.N. from the U. S. Department of Energy, Grant No. DE-FG02-08ER15957 from the Chemical Sciences, Geosciences and Biosciences Division, Office of Basic Energy Sciences and the National Science Foundation (Subaward No. 12-764). O.B.O. and D.S. were supported by Fellowship Awards from the Rutgers University Aresty Research Center for Undergraduates.

References

[1] C.N. Hunter, F. Daldal, M.C. Thurnauer, J.T. Beatty (Eds.), The Purple Phototrophic Bacteria, Springer, Netherlands, Dordrecht, 2008.
[2] G. Drews, R.A. Niederman, Membrane biogenesis in anoxygenic photosynthetic prokaryotes, Photosynth. Res. 73 (2002) 87–94.
[3] M. Koblízek, J.D. Shih, S.I. Breitbart, E.C. Ratcliffe, Z.S. Kolber, C.N. Hunter, R.A. Niederman, Sequential assembly of photosynthetic units in *Rhodobacter sphaeroides* as revealed by fast repetition rate analysis of variable bacteriochlorophyll *a* fluorescence, Biochim. Biophys. Acta 1706 (2005) 220–231.
[4] R.A. Niederman, Structure, function and formation of bacterial intracytoplasmic membranes, in: J.M. Shively (Ed.), Complex Intracellular Structures in Prokaryotes, Microbiology Monographs, vol. 2, Springer, Germany, Berlin 2006, pp. 193–227.
[5] R.A. Niederman, Membrane development in purple photosynthetic bacteria in response to alterations in light intensity and oxygen tension, Photosynth. Res. 116 (2013) 333–348.
[6] X. Zeng, J.H. Roh, S.J. Callister, C.L. Tavano, T.J. Donohue, M.S. Lipton, S. Kaplan, Proteomic characterization of the *Rhodobacter sphaeroides* 2.4.1 photosynthetic membrane: identification of new proteins, J. Bacteriol. 189 (2007) 7464–7474.
[7] K. Woronowicz, R.A. Niederman, Proteomic analysis of the developing intracytoplasmic membrane in *Rhodobacter sphaeroides* during adaptation to low light intensity, Adv. Exp. Med. Biol. 675 (2010) 161–178.
[8] K. Woronowicz, D. Sha, R.N. Frese, R.A. Niederman, The accumulation of the light-harvesting 2 complex during remodeling of the *Rhodobacter sphaeroides* intracytoplasmic membrane results in a slowing of the electron transfer turnover rate of photochemical reaction centers, Biochemistry 50 (2011) 4819–4829.
[9] K. Woronowicz, D. Sha, R.N. Frese, J.N. Sturgis, V. Nanda, R.A. Niederman, The effects of protein crowding in bacterial photosynthetic membranes on the flow of quinone redox species between the photochemical reaction center and the ubiquinol-cytochrome c_2 oxidoreductase, Metallomics 3 (2011) 765–774.
[10] K. Woronowicz, O.B. Olubanjo, H.C. Sung, J.L. Lamptey, R.A. Niederman, Differential assembly of polypeptides of the light-harvesting 2 complex encoded by distinct operons during acclimation of *Rhodobacter sphaeroides* to low light intensity, Photosynth. Res. 108 (2011) 201–214.
[11] R.A. Niederman, Eukaryotic behaviour of a prokaryotic energy transducing membrane: fully detached vesicular organelles arise by budding from the *Rhodobacter sphaeroides* intracytoplasmic photosynthetic membrane, Mol. Microbiol. 76 (2010) 803–805.
[12] P.G. Heytler, Uncoupling of oxidative phosphorylation by carbonyl cyanide phenylhydrazones. I. Some characteristics of m-Cl-CCP action on mitochondria and chloroplasts, Biochemistry 2 (1963) 357–361.
[13] J. Cunarro, M.W. Weiner, Mechanism of action of agents which uncouple oxidative phosphorylation: direct correlation between proton-carrying and respiratory-releasing properties using rat liver mitochondria, Biochim. Biophys. Acta 387 (1975) 234–240.
[14] R. Dierstein, G. Drews, Effect of uncoupler on assembly pathway for pigment-binding protein of bacterial photosynthetic membranes, J. Bacteriol. 168 (1986) 167–172.
[15] G. Drews, Formation of the light-harvesting complex I (B870) of anoxygenic phototrophic purple bacteria, Arch. Microbiol. 166 (1996) 151–159.
[16] M. Meryandini, G. Drews, Import and assembly of the α- and β-polypeptides of the light-harvesting complex I (B870) in the membrane system of *Rhodobacter capsulatus* investigated in an *in vitro* translation system, Photosynth. Res. 47 (1996) 21–31.
[17] J. Komenda, V. Reisinger, B.C. Müller, Accumulation of the D2 protein is a key regulatory step for assembly of the photosystem II reaction center complex in *Synechocystis* PCC 6803, J. Biol. Chem. 279 (2004) 48620–48629.
[18] M. Dobáková, R. Sobotka, M. Tichý, J. Komenda, Psb28 protein is involved in the biogenesis of the photosystem II inner antenna CP47 (PsbB) in the cyanobacterium *Synechocystis* sp. PCC 68031, Plant Physiol. 149 (2009) 1076–1086.
[19] J. Komenda, J. Knoppová, J. Kopečná, R. Sobotka, P. Halada, J. Yu, J. Nickelsen, M. Boehm, P.J. Nixon, The Psb27 assembly factor binds to the CP43 complex of photosystem II in the cyanobacterium *Synechocystis* sp. PCC 68031, Plant Physiol. 158 (2012) 476–486.
[20] G. Drews, The intracytoplasmic membranes of purple bacteria — assembly of energy transducing complexes, J. Mol. Microbiol. Biotechnol. 23 (2013) 35–47.
[21] J.N. Sturgis, R.A. Niederman, Organization and assembly of light-harvesting complexes in the purple bacterial membrane, in: C.N. Hunter, F. Daldal, M.C. Thurnauer, J.T. Beatty (Eds.), The Purple Phototrophic Bacteria, Springer, Netherlands, Dordrecht 2008, pp. 253–273.
[22] K. Woronowicz, J.W. Harrold, J.M. Kay, R.A. Niederman, Structural and functional proteomics of intracytoplasmic membrane assembly in *Rhodobacter sphaeroides*, J. Mol. Microbiol. Biotechnol. 23 (2013) 48–62.
[23] I. Wittig, M. Karas, H. Schägger, High resolution clear native electrophoresis for in-gel functional assays and fluorescence studies of membrane protein complexes, Mol. Cell. Proteomics 6 (2007) 1215–1225.
[24] D.E. Sleat, L. Ding, S. Wang, C. Zhao, Y. Wang, W. Xin, H. Zheng, D.F. Moore, K.B. Sims, P. Lobel, Mass spectrometry-based protein profiling to determine the cause of lysosomal storage diseases of unknown etiology, Mol. Cell. Proteomics 8 (2009) 1708–1718.
[25] C. Mackenzie, M. Choudhary, F.W. Larimer, P.F. Predki, S. Stilwagen, J.P. Armitage, R.D. Barber, T.J. Donohue, J.P. Hosler, J.E. Newman, J.P. Shapleigh, R.E. Sockett, J. Zeilstra-Ryalls, S. Kaplan, The home stretch, a first analysis of the nearly completed genome of *Rhodobacter sphaeroides* 2.4.1, Photosynth. Res. 70 (2001) 19–41.
[26] G.M. D'Amici, S. Rinalducci, L. Murgiano, F. Italiano, L. Zolla, Oligomeric characterization of the photosynthetic apparatus of *Rhodobacter sphaeroides* R26.1 by nondenaturing electrophoresis methods, J. Proteomic Res. 9 (2010) 192–203.
[27] M. Kis, E. Asztalos, G. Sipka, P. Maróti, Assembly of photosynthetic apparatus in *Rhodobacter sphaeroides* as revealed by functional assessments at different growth phases and in synchronized and greening cells, Photosynth. Res. 122 (2014) 261–273.
[28] E. Papagiannakis, J.T.M. Kennis, I.H.M. van Stokkum, R.J. Cogdell, R. van Grondelle, An alternative carotenoid-to-bacteriochlorophyll energy transfer pathway in photosynthetic light harvesting, Proc. Natl. Acad. Sci. U. S. A. 99 (2002) 6017–6022.
[29] S. Bahatyrova, R.N. Frese, C.A. Siebert, K.O. van der Werf, R. van Grondelle, R.A. Niederman, P.A. Bullough, C. Otto, J.D. Olsen, C.N. Hunter, The native architecture of a photosynthetic membrane, Nature 430 (2004) 1058–1062.
[30] C.N. Hunter, J.D. Pennoyer, J.N. Sturgis, D. Farrelly, R.A. Niederman, Oligomerization states and associations of light-harvesting pigment-protein complexes of *Rhodobacter sphaeroides* as analyzed by lithium dodecyl sulfate-polyacrylamide gel electrophoresis, Biochemistry 27 (1988) 3459–3467.
[31] R.L. Tatusov, E.V. Koonin, D.J. Lipman, A genomic perspective on protein families, Science 278 (1997) 631–637.
[32] J.N. Sturgis, C.N. Hunter, R.A. Niederman, Spectra and extinction coefficients of near-infrared absorption bands in membranes of *Rhodobacter sphaeroides* mutants lacking light-harvesting and reaction center complexes, Photochem. Photobiol. 48 (1988) 243–247.
[33] C.N. Hunter, J.D. Tucker, R.A. Niederman, The assembly and organisation of photosynthetic membranes in *Rhodobacter sphaeroides*, Photochem. Photobiol. Sci. 4 (2005) 1023–1027.
[34] J.D. Tucker, C.A. Siebert, M. Escalante, P.G. Adams, J.D. Olsen, C. Otto, D.L. Stokes, C.N. Hunter, Membrane invagination in *Rhodobacter sphaeroides* is initiated at curved regions of the cytoplasmic membrane, then forms both budded and fully detached spherical vesicles, Mol. Microbiol. 76 (2010) 833–847.
[35] M.L. Cartron, J.D. Olsen, M. Sener, P.J. Jackson, A.A. Brindley, P. Qian, M.J. Dickman, G.J. Leggett, K. Schulten, C.N. Hunter, Integration of energy and electron transfer processes in the photosynthetic membrane of *Rhodobacter sphaeroides*, Biochim. Biophys. Acta 1837 (2014) 1769–1780.
[36] P. Joliot, A. Joliot, A. Verméglio, Fast oxidation of the primary electron acceptor under anaerobic conditions requires the organization of the photosynthetic chain of *Rhodobacter sphaeroides* in supercomplexes, Biochim. Biophys. Acta 1706 (2005) 204–214.
[37] P.J. Jackson, H.J. Lewis, J.D. Tucker, C.N. Hunter, M.J. Dickman, Quantitative proteomic analysis of intracytoplasmic membrane development in *Rhodobacter sphaeroides*, Mol. Microbiol. 84 (2012) 1062–1067.
[38] P.L. Sorgen, M.R. Bubb, K.A. McCormick, A.S. Edison, B.D. Cain, Formation of the b subunit dimer is necessary for interaction with F_1-ATPase, Biochemistry 37 (1998) 923–932.
[39] S. Ahmad, N.A. Glavas, P.D. Bragg, Assembly of multimeric proteins. Effect of mutations in the alpha-subunit on membrane assembly and activity of pyridine nucleotide transhydrogenase, J. Mol. Biol. 234 (1993) 8–13.
[40] J. Bachmann, B. Bauer, K. Zwicker, B. Ludwig, O. Anderka, The Rieske protein from *Paracoccus denitrificans* is inserted into the cytoplasmic membrane by the twin-arginine translocase, FEBS J. 273 (2006) 4817–4830.
[41] C. Breyton, W. Haase, T.A. Rapoport, W. Kuhlbrandt, I. Collinson, Three-dimensional structure of the bacterial protein-translocation complex SecYEG, Nature 418 (2002) 662–665.
[42] J.C. Samuelson, M. Chen, F. Jiang, I. Moller, M. Wiedmann, A. Kuhn, G.J. Phillips, R.E. Dalbey, YidC mediates membrane protein insertion in bacteria, Nature 406 (2000) 637–641.
[43] I. Sachelaru, N.A. Petriman, R. Kudva, P. Kuhn, T. Welte, B. Knapp, F. Drepper, B. Warscheid, H.-G. Koch, YidC occupies the lateral gate of the SecYEG translocon and is sequentially displaced by a nascent membrane protein, J. Biol. Chem. 288 (2013) 16295–16307.
[44] L. Zhu, H.R. Kaback, R.E. Dalbey, YidC protein, a molecular chaperone for LacY protein folding via the SecYEG protein machinery, J. Biol. Chem. 288 (2013) 28180–28194.
[45] L. Yi, F. Jiang, M. Chen, B. Cain, A. Bolhuis, R.E. Dalbey, YidC is strictly required for membrane insertion of subunits a and c of the F_1F_0ATP synthase and SecE of the SecYEG translocase, Biochemistry 42 (2003) 10537–10544.

[46] M. Van Der Laan, M.L. Urbanus, C.M. Ten Hagen-Jongman, N. Nouwen, B. Oudega, N. Harms, A.J. Driessen, J. Luirink, A conserved function of YidC in the biogenesis of respiratory chain complexes, Proc. Natl. Acad. Sci. U. S. A. 100 (2003) 5801–5806.
[47] N. Nouwen, A.J. Driessen, SecDFYajC forms a heterotetrameric complex with YidC, Mol. Microbiol. 44 (2002) 1397–1405.
[48] R.J. Schulze, J. Komar, M. Botte, W.J. Allen, S. Whitehouse, V.A. Gold, A. Lycklama, J.A. Nijehol, K. Huard, I. Berger, C. Schaffitzel, I. Collinson, Membrane protein insertion and proton-motive-force-dependent secretion through the bacterial holotranslocon SecYEG–SecDF-YajC–YidC, Proc. Natl. Acad. Sci. U. S. A. 111 (2014) 4844–4849.
[49] S.E. Lang, F.E. Jenney, F. Daldal, *Rhodobacter capsulatus* CycH: a bipartite gene product with pleiotropic effects on the biogenesis of structurally different *c*-type cytochromes, J. Bacteriol. 178 (1996) 5279–5290.
[50] C.S. Young, J.T. Beatty, Multi-level regulation of purple bacterial light-harvesting complexes, in: B.R. Green, W.W. Parson (Eds.), Light-Harvesting Antennas in Photosynthesis, Kluwer Academic Publishers, Dordrecht, The Netherlands 2003, pp. 449–470.
[51] K. Ito, Y. Akiyama, Cellular functions, mechanism of action, and regulation of FtsH protease, Annu. Rev. Microbiol. 59 (2005) 211–231.
[52] E. van Bloois, H.L. Dekker, L. Froderberg, E.N.G. Houben, M.L. Urbanus, C.G. de Koster, J.-W. de Gier, J. Luirink, Detection of cross-links between FtsH, YidC, HflK/C suggests a linked role for these proteins in quality control upon insertion of bacterial inner membrane proteins, FEBS Lett. 582 (2008) 1419–1424.
[53] N. Tavernarakis, M. Driscoll, N.C. Kyrpides, The SPFH domain: implicated in regulating targeted protein turnover in stomatins and other membrane-associated proteins, Trends Biochem. Sci. 24 (1999) 425–427.
[54] J. Luirink, I. Sinning, SRP-mediated protein targeting: structure and function revisited, Biochim. Biophys. Acta 1694 (2004) 17–35.
[55] M. Paetzel, R.E. Dalbey, N.C. Strynadka, Crystal structure of a bacterial signal peptidase in complex with a beta-lactam inhibitor, Nature 396 (1998) 186–190.
[56] J.D. Olsen, P.G. Adams, P.J. Jackson, M.J. Dickman, P. Qian, C.N. Hunter, Aberrant assembly complexes of the reaction center light-harvesting 1 PufX (RC-LH1-PufX) core complex of *Rhodobacter sphaeroides* imaged by atomic force microscopy, J. Biol. Chem. 289 (2014) 29927–29936.
[57] P. Freestone, M. Trinei, S.C. Clarke, T. Nyström, V. Norris, Tyrosine phosphorylation in *Escherichia coli*, J. Mol. Biol. 279 (1998) 1045–1051.
[58] L. Nachin, U. Nannmark, T. Nyström, Differential roles of the universal stress proteins of *Escherichia coli* in oxidative stress resistance, adhesion, and motility, J. Bacteriol. 187 (2005) 6265–6272.
[59] S.Y. Kim, E.J. Miller, J. Frydman, W.E. Moerner, Action of the chaperonin GroEL/ES on a non-native substrate observed with single-molecule FRET, J. Mol. Biol. 401 (2010) 553–563.